Nanoparticle-Enabled Selective Electrodeposition

Hsien-Ping Feng, Trilochan Paudel, Bo Yu, Shuo Chen, Zhi Feng Ren, and Gang Chen**

Electroplating is a common process used in a wide range of industries. For example, electroplated copper and copper-based alloys are used in ultralarge-scale integration devices requiring multilevel metallization.[1,2] Electroplating has more recently been used in optoelectronic components, such as transparent thin-film transistors, flat panel displays, light-emitting diodes, photovoltaic cells, and electrochromic windows, where substrates are typically semiconductors (GaAs) or transparent conductive oxides (TCOs, e.g., zinc oxide, indium tin oxide, and fluorine-doped tin oxide).[3,4] However, metallization directly on glass and other low-roughness ceramics is difficult because the smooth interface does not provide opportunities to interlock at the interface between the substrate and the materials to be plated.[5] Accordingly, prior to electroplating, etching is commonly used to increase surface roughness, followed by sputtering a thin adhesive layer (such as titanium) to improve adhesion. For electroplating metallization, the key is the nucleation process, which is determined by the formation energy, excess energy, and internal strain energy.[6–9] In general, a smooth and hydrophobic semiconductor surface, such as silicon, gallium arsenide, or transparent conductive glass, has low surface energy and poor wettability, leading to a relatively high excess energy for electroplating nucleation. As a consequence, scattered and irregular grains grow on a small number of nucleation sites, causing poor interface adhesion and large surface roughness. Strain energy, originating from the different atomic arrangement of the two adjacent layers, increases with increasing film thickness and can sometimes cause the film to spontaneously peel off.

In many applications, it is relatively common to electroplate metal over an entire surface of a base conductor even though only small areas of the metal are needed on the surface. The use of electroplating in this context typically consists of a patterning process followed by a metallization process. Photolithography is the most popular method to create such patterns where a photoresist is used as the patterning layer.[10,11] The metallization process typically consists of sputtering, electroplating, and chemical mechanical polishing. Metal is first sputtered onto the patterned regions, which improves both the adhesion and electrical conductivity of the primary structure, particularly for smooth semiconductor surfaces. Electroplating is then used to construct the primary structure followed by chemical mechanical polishing to remove any surplus metal, planarizing the entire surface. Then, the photoresist from the patterning process is removed. For material savings, the use of the selective electroplating has been recognized for years. Prior techniques, such as doping patterns on the substrate or a high-speed electrolyte jet system, that were developed for selective electroplating aim to reduce the quantities of metal used, but require costly specialized equipment and result in reduced production rates.[12–14]

This paper reports a method to overcome the difficulties of electroplating on low-surface-energy substrates by using immobilized platinum nanoparticles that strongly adhere to the substrate to serve as nucleation sites. A wide array of nanoparticle materials can also be used. The effectiveness of the approach is demonstrated on TCO substrates for which conventional electroposition leads to weak bonding between the metal and the substrates. We discovered that these nanoparticle seed layers also open up a voltage range so that metals can be selectively deposited onto the nanoparticle-seeded regions only, thus providing new routes for selective area deposition. The submicrometer metallic pattern can be selectively electroplated onto the predetermined nanoparticle area, which is demonstrated with the aid of patterned areas by a nanosphere lithography technique.

Figure 1A shows a cathodic wave from cyclic voltammetry for nickel on fluorine-doped tin oxide (FTO) with and without platinum nanoparticles. A Gamry PCI4/300 potentistat/galvanostat was used in the electrochemical measurement in a standard three-electrode system with a platinum mesh as the counter electrode and a saturated calomel electrode (SCE) as the reference electrode. As shown, the current–potential curve of nickel on FTO glass pretreated with nanoparticles became less negative than the blank surface. A similar trend can be observed in electroplated copper, tin, and gold, as shown in Figure 1B–D. As shown, electrodeposition on a nanoparticle-pretreated surface all occurs at a less negative potential. Nickel electrodeposition onto a bulk platinum surface requires a less negative onset potential (–0.75 V) (Figure 1A) compared to the blank FTO surface (–1.0 V), which indicates that atomic clusters bond more strongly on platinum. Furthermore, nickel deposited on platinum nanoparticles have a less negative onset potential (–0.53 V) than that on a bulk platinum surface. This is because nanosized platinum particles have high surface energy, and thus serve as nucleation sites for atomic clusters to preferentially deposit on them to reduce the total surface energy.[15,16] The deposited atoms will be more strongly bound to the nanoparticles, which were strongly immobilized onto the substrate, leading to stronger adhesion. Pull-off adhesion tests for electroplated metals (nickel, copper, tin, and gold) on FTO glass with the nanoparticle treatment showed that no coating was stripped

Dr. H. P. Feng, Dr. S. Chen, Prof. G. Chen
Department of Mechanical Engineering
Massachusetts Institute of Technology
Cambridge, MA 02139, USA
E-mail: gchen2@mit.edu
T. Paudel, B. Yu, Prof. Z. F. Ren
Department of Physics
Boston College, Chestnut Hill, MA 02467, USA
E-mail: renzh@bc.edu

DOI: 10.1002/adma.201004656

© 2011 WILEY-VCH Verlag GmbH & Co. KGaA, Weinheim

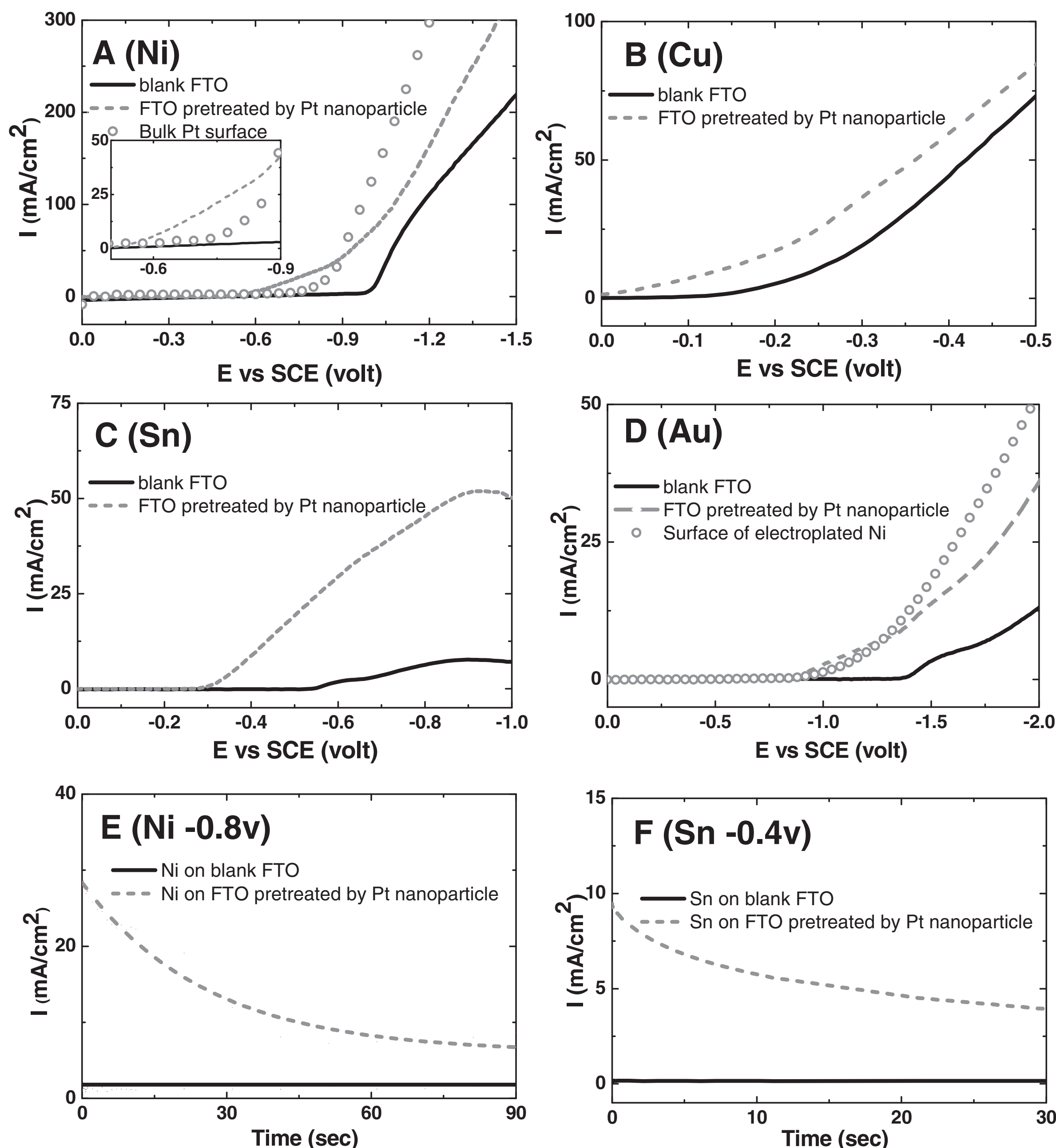

Figure 1. Cathodic waves of cyclic voltammetry for A) nickel, B) copper, C) tin, and D) gold electroplated on FTO with and without platinum nanoparticles. Chronoamperograms of electroplating E) nickel under operating voltage of –0.8 V and F) tin under operating voltage of –0.4 V.

off by 3M flatback Mmsking tape 250 (ASTM D3359). In contrast, without nanoparticle treatment, almost all of the coating on the blank FTO glass was removed (see Supporting Information Figure S1).

As shown in the inset of Figure 1A, it opens an operation window for selective electroplating where only areas seeded with nanoparticles will be electroplated (See Supporting Information Figure S2). For example, the nickel electroplated on blank FTO surfaces requires a larger onset potential of $E_{\text{onset}} = -1.0$ V to initiate deposition when compared to the FTO surface with nanoparticle treatment ($E_{\text{onset}} = -0.53$ V). The chronoamperograms in Figure 1E show the current response to the optimum operating voltage at –0.8 V for electroplating nickel on FTO with and without platinum nanoparticle treatment. The average rate of electroplating nickel on FTO with the Pt nanoparticle treatment was about 0.2 μm min^{-1} (as measured by a profilometer) while almost no faradic current could be detected for electroplating on blank FTO, which verifies the above-mentioned mechanism. Consistent results can be seen in the chronoamperograms for electroplated tin under operating voltage of –0.4 V (Figure 1F) (Supporting Information Figure S3). Additionally, the gray circles curve of Figure 1D corresponds to gold deposited onto

© 2011 WILEY-VCH Verlag GmbH & Co. KGaA, Weinheim

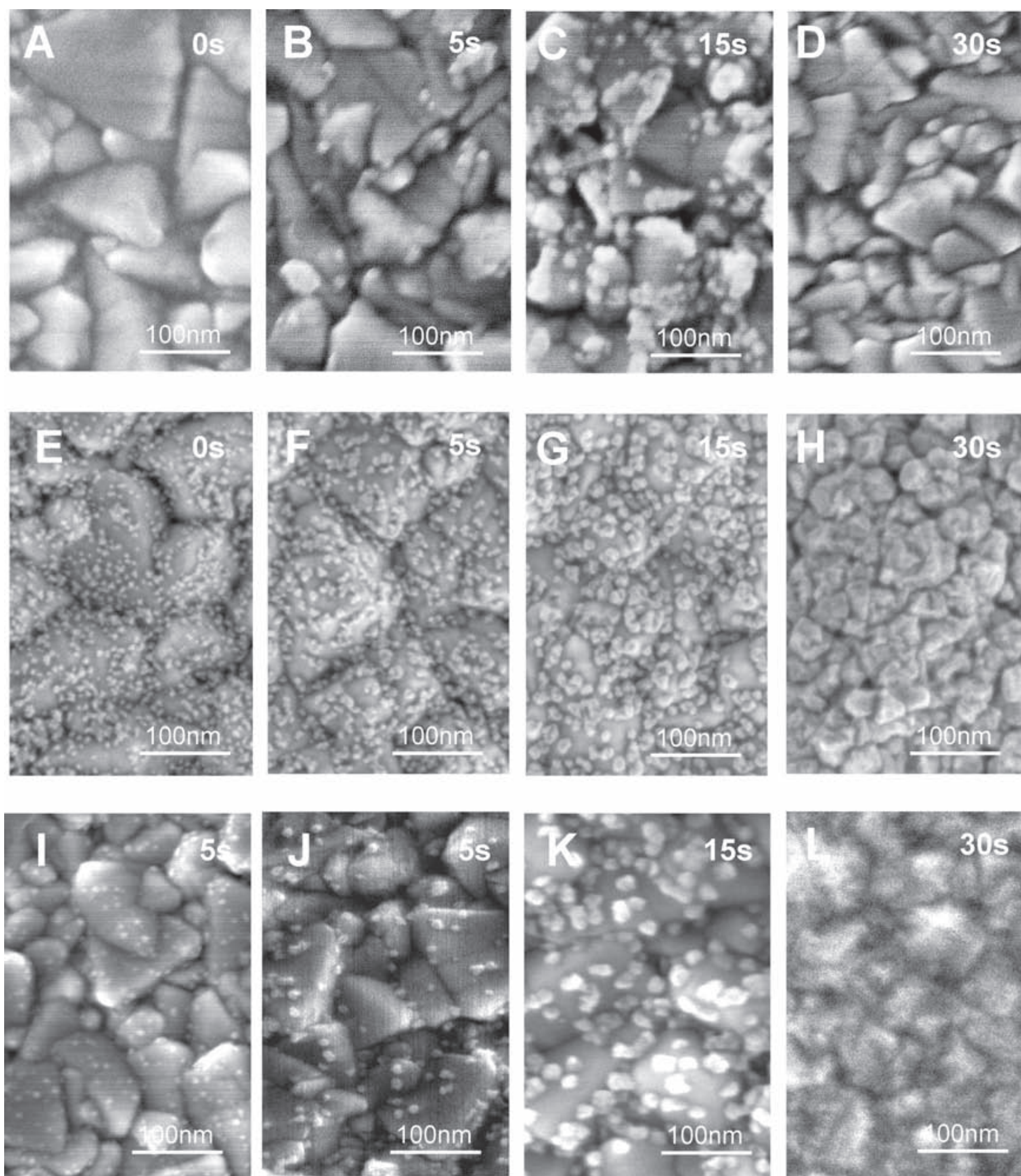

Figure 2. SEM images of nickel electroplated 0, 5, 15, and 30 s on a blank FTO surface (A–D), on a FTO surface pretreated by platinum nanoparticles (E–H), and on a FTO surface covered with 20% diluted platinum nanoparticles (I–L).

nickel, which was originally electroplated on the nanoparticle regions. As seen, it also becomes more positive compared with electroplated gold on blank FTO, thus creating a second operation window for the selective electroplating of gold. The reason could be that better wettability on electroplated nickel results in a lower excess energy for electroplating.[6,8] Thus, theoretically, a double-layer structure can also be achieved by this method.

Figures 2A–D are scanning electron microscopy (SEM) images of 100-nm electroplated nickel on blank FTO at 0, 5, 15, and 30 s. Generally, for smooth semiconductor surfaces, the excess free energy of nucleation taking into account new phases being generated from the bulk phase is rather high. Thus, the early stage of the electrochemical phase transformation corresponds to an instantaneous nucleation model, where the growth of nuclei on a small number of active sites, such as atomic step, grain edge, crystal defects, and impurities, occurs in a very short time period. These nucleation sites grow into islands and then coalesce (Volmer–Weber growth).[15,17] Island growth during electroplating nucleation is usually not desirable for technological applications due to its poor adhesion and non-uniform deposition. As seen, the uneven and random distribution of a few active sites would cause irregular

© 2011 WILEY-VCH Verlag GmbH & Co. KGaA, Weinheim

grain size to increase film roughness. Uneven grain growth also leads to stacking faults, increasing film stress and strain due to a mismatch in the lattice spacing. Therefore, the poor adhesion can be understood by weak interface contact and large strain and stress in the electroplated film. Figure 2E–H show electroplating nickel at 0, 5, 15, and 30 s on a FTO surface pretreated with platinum nanoparticles. When operating within the optimum range for selective electroplating, all nickel atoms nucleated and grew onto nanoparticles. A conformable nickel film with a uniform grain size on average of 30 nm can be achieved. Within the process window for selective electroplating, it is also possible to control the grain size by the density of nanoparticles. To show this, we diluted the nanoparticle solution to 20% to reduce the number of nanoparticles on the FTO surface. Figure 2I–L show electroplated nickel at 0, 5, 15, and 30 s on a FTO surface with a reduced number of platinum nanoparticles. Again, all nickel atoms were electroplated onto a small number of nanoparticles in order to minimize the surface energy and then coalesced until a grain structure was formed with an average size of 75 nm. **Figure 3** is an atomic force microscopy (AFM) image of 100-nm nickel on blank FTO glass. The root mean square of roughness increases over two-fold after electroplating nickel (Figure 3A,B). Figure 3C shows the AFM image of electroplated nickel on FTO glass with the nanoparticle treatment. Its root mean square of roughness is almost the same as the blank substrate because the nanoparticle monolayer serves as an even nucleation layer. In summary, the method of immobilizing nanoparticles onto the substrate provides a good adhesive nucleated layer to produce a reliable and uniform electroplated film.

As mentioned above, a patterned structure can be achieved by patterning the immobilized nanoparticle on the substrate. The nanoparticle pattern can be defined using many processes, including photolithography, screen printing, inkjet technology, microcontact stamp printing, dip-pen nanolithography, and electrochemical imprinting.[18,19] To demonstrate the principle, a low-cost patterning technique based on self-assembled polystyrene microspheres was chosen here to prepare highly ordered dot arrays.[20–22] **Figure 4** is a process flow diagram detailing the creation of a patterned metallic layer on a substrate. The related processing conditions are given in the Experimental Section.

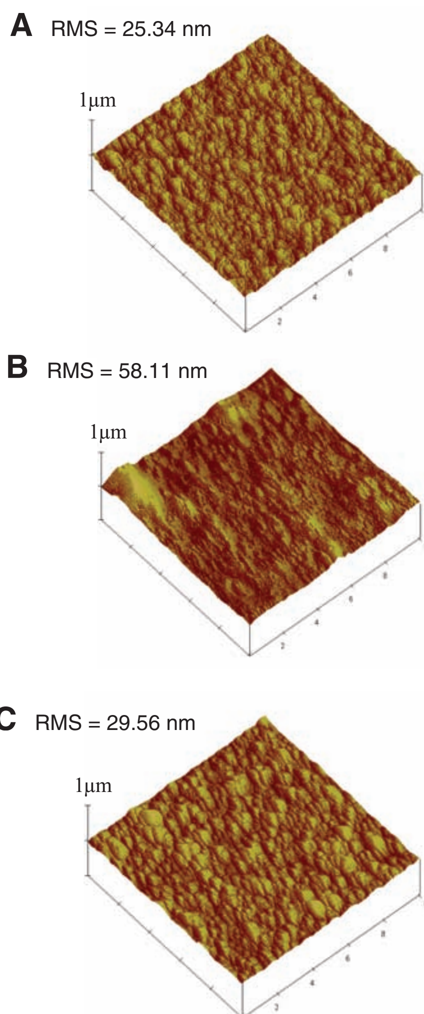

Figure 3. AFM images of A) a blank FTO surface and 100-nm nickel electroplated on FTO surface B) without and C) with Pt nanoparticle treatment. The AFM scan size was 10 μm and the scan rate was 1 Hz. The *Z*-axes for the height are 1 μm per div and *X*-axes are 2 μm per div. RMS is the root mean square of the roughness.

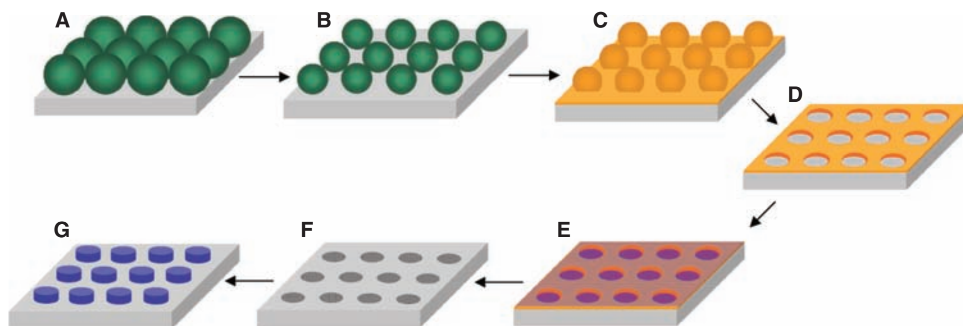

Figure 4. The sequence of steps for selective electroplating a patterned metallic layer on a substrate. A) A monolayer of polystyrene microspheres on a FTO surface. B) Inductively coupled plasma reactive ion etching (ICP-RIE) with oxygen. C) Electron beam evaporation of a 150-nm Cu layer as a sacrificed mask. D) Polystyrene spheres are removed, leaving holes at the original position of the spheres. E) Immersion into a 1% ML-371 at 45 °C for 5 min. F) Immersion into a solution of polyvinylpyrrolidone (PVP)-capped Pt nanoclusters suspended at room temperature for 5 min and then annealed at 250 °C for 15 min. G) Metallization at an operation window for selectively electroplating.

© 2011 WILEY-VCH Verlag GmbH & Co. KGaA, Weinheim

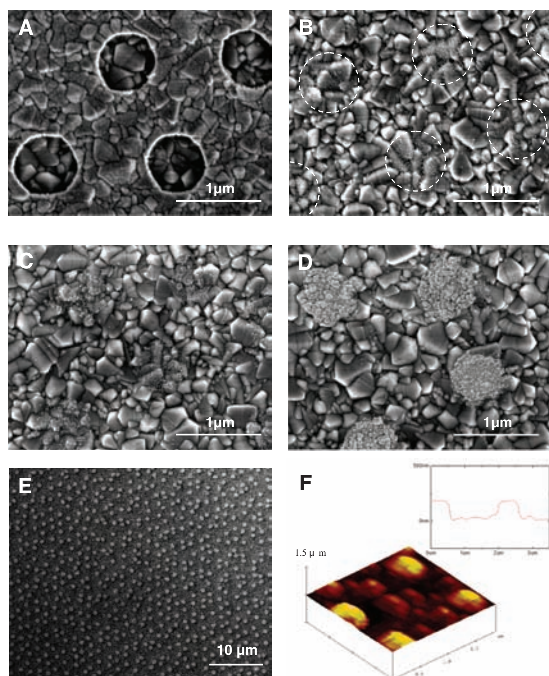

Figure 5. SEM images of A) a continuous Cu network and opening holes on FTO surface after removing the spheres; B) self-assembly patterned arrays of platinum nanoparticles, electroplated nickel at operating voltage of –0.8 V for C) 15 s and D) 60 s; and E) a zoomed-out image of the nickel dots on FTO surface. F) AFM image of nickel dots on a FTO surface. The inset shows the corresponding line scan.

Figure 5A shows SEM images of the opening holes in a range of 500 to 700 nm. Nanoparticle dot patterns can be generated on the substrate after immersion into a nanoparticle solution and annealing treatment, as shown in Figure 5B. The nickel is then electroplated at an operating voltage of –0.8 V for 15 s (Figure 5C) and 60 s (Figure 5D) to yield metal islands on predetermined nanoparticle areas. As shown in Figure 5E, nickel dot arrays have an average diameter of 600 nm and are spaced 1 μm apart. Figure 5F shows an AFM image and a corresponding line scan of a pattern, which demonstrates that the feature of metal dots in the thickness of 200 nm has been developed cleanly on FTO surface.

In summary, we invented an electrodeposition process using nanoparticles as seed layers. The nanoparticle monolayer not only provides a good adhesive layer but also an even nucleation site for electroplating to achieve improved adhesion and uniformity. The electroplated film is smooth and may not require chemical mechanical polishing afterward. The control of the grain size is also achievable by this new method and will be of fundamental interest for studying the characteristics of electrodeposition. The nanoparticle seed layer also opens up a voltage window for selective area deposition into the region seeded with nanoparticles only. Nanoparticle deposition onto selected regions can be done via many established methods, such as lithography, microcontact stamp printing, and dip-pen nanolithography. Thus, the process would be applicable in the manufacturing of various micro- and nanostructures. We demonstrate this potential using nanosphere lithography.

Experimental Section

Process of Seeding Nanoparticles: The experiments were carried out using an electroplated metal (nickel, copper, tin, or gold) on FTO with and without the platinum-nanoparticle treatment. Here, platinum nanoparticles were chosen because platinum is an inert metal and its suspension is readily prepared without additional purification.[23,24] Although we only use platinum nanoparticles in this work, a wide array of nanoparticle materials can also be used. FTO glass, 1 cm^2 square and 2 mm thick, have a sheet resistance of 10 $\Omega\ \square^{-1}$, resistivity of 350 μΩ cm, a band ap of 3.8 eV, and optical transmission of 90%. Before nanoparticle deposition and electroplating, the FTO glass was immersed in a 2% PK-LCG545 (Parker Corp.) at 50 °C for 5 min with sonication to clean the surface. A platinum nanoparticle monolayer was deposited onto a FTO surface by immersion into a 1% surface conditioner (2-(2-aminoethylamino) ethanol, AEEA) at 45 °C for 5 min and then a solution of PVP-capped Pt nanoclusters suspension at room temperature for 5 min.[25,26] The pretreated surface was then annealed at 250 °C for 10 min under ambient conditions in order to sinter the platinum nanoparticles and burn the protective PVP polymer away. Nickel was then electroplated onto the pretreated surface within an optimum range of the operating voltage from a commercial electrolyte at 53 °C. These processes were then reproduced on electroplated copper, tin, and gold at room temperature. It should be noted that insufficient annealing time caused poor bonding between the nanoparticles and the substrate leading to poor adhesion (Supporting Information Figure S4).

Fabrication of Self-Aligned Platinum Nanoparticle Patterns: The process is shown in Figure 4. A self-assembled monolayer of 1.5-μm polystyrene microspheres on an aqueous surface was transferred onto the FTO surface.[21] The diameters of the polystyrene beads were tailored by ICP-RIE with 50 sccm oxygen and 5 sccm tetrafluoromethane at a pressure of 100 mTorr and radio frequency (RF) power of 100 W with a 480 s etching time.[22] A 150-nm Cu layer was deposited as a sacrificed mask by electron beam evaporation at room temperature. The spheres were completely removed by ultrasonication in tetrahydrofuran, leaving holes at the original position of the spheres. The substrate was immersed into a 1% ML-371 at 45 °C for 5 min and then a solution of PVP-capped Pt nanoclusters suspension (pH = 2.3) at room temperature for 5 min. A nanoparticle dot pattern could be self-aligned on FTO surface due to the platinum nanoparticles that were adhered by ML-371 surfactant on opening holes and the Cu layer was simultaneously dissolved in acid PVP-Pt solution. The nanoparticle pattern was then immobilized on the substrate via 250 °C for 15 min annealing. Finally, the desired substance could be selectively electroplated onto the predetermined nanoparticle area at an operating voltage within the optimum range.

Supporting Information

Supporting Information is available from the Wiley Online Library or from the author.

Acknowledgements

The authors thank Dr. S. Shen for very helpful discussions, Jonathan K. Tong for editorial assistance, and the Postdoctoral Research Abroad Program supported by National Science Council of Republic of China, Taiwan. This work is supported partially as part of the "Solid State Solar-Thermal Energy Conversion Center" (S3TEC), an Energy Frontier Research Center funded by the U.S. Department of Energy, Office of Science, Office of Basic Energy Sciences under Award Number: DE-SC0001299 (G.C. and Z.F.R.).

Received: December 19, 2010
Revised: February 14, 2011
Published online: May 3, 2011

© 2011 WILEY-VCH Verlag GmbH & Co. KGaA, Weinheim

[1] J. Škriniarová, J. Jakabovič, I. Kostič, *J. Electr. Eng.* **2004**, *55*, 43.
[2] H. C. Chen, M. S. Yang, J. Y. Wu, W. Lur, *Proc. IEEE Int. Interconnect Technol. Conf.* **1999**, 65.
[3] L. Y. Chen, H. I. Chen, C. C. Huang, Y. W. Huang, T. H. Tsai, Y. C. Liu, T. Y. Chen, S. Y. Cheng, W. C. Liu, *Appl. Phys. Lett.* **2009**, *95*, 052105.
[4] M. Nakao, J. Kumaki, K. Matsumoto, Y. Hatamura, *Precis. Eng.* **2004**, *28*, 181.
[5] M. Charbonnier, M. Romand, *Surf. Coat. Technol.* **2002**, *162*, 19.
[6] D. Walton, *Nucleation*, Decker, New York **1969**.
[7] G. Staikov, E. Budevski, M. Hőpfner, W. Obretenov, K. Jűttner, W. J. Lorenz, *Surf. Sci.* **1991**, *248*, 234.
[8] D. Grujicic, B. Pesic, *Electrochim. Acta* **2002**, *47*, 2901.
[9] E. Budevski, G. Staikov, W. J. Lorenz, *Electrochim. Acta* **2000**, *45*, 2559.
[10] L. Dellmann, S. Roth, C. Beuret, G.-A. Racine, H. Lorenz, M. Despont, P. Renaud, P. Vettiger, N. F. de Rooij, *Sens. Actuators A* **1998**, *70*, 42.
[11] H. S. Shin, J. Y. Song, J. Yu, *Mater. Lett.* **2009**, *63*, 397.
[12] E. D. Herderick, J. S. Tresback, A. L. Vasiliev, N. P. Padture, *Nanotechnology* **2007**, *18*, 155204.
[13] K. Sugioka, K. Toyoda, Y. Gomi, S. Tanaka, *Appl. Phys. Lett.* **1989**, *55*, 619.
[14] C. Scheck, P. Evans, R. Schad, G. Zangari, L. Sorba, G. Biasiol, S. Heun, *Appl. Phys. Lett.* **2005**, *86*, 133108.
[15] V. M. Kaganer, B. Jenichen, R. Shayduk, W. Braun, H. Riechert, *Phys. Rev. Lett.* **2009**, *102*, 016103.
[16] S. S. Coffee, J. G. Ekerdt, *J. Appl. Phys.* **2007**, *102*, 114912.
[17] M. Miyamoto, S. Hirano, H. Chibahara, T. Watadani, M. Akazawa, S. Furukawa, *Jpn. J. Appl. Phys.* **2006**, *45*, 7637.
[18] V. Santhanam, R. P. Andres, *Nano Lett.* **2004**, *4*, 41.
[19] W. M. Wang, R. M. Stoltenberg, S. Liu, Z. Bao, *ACS Nano* **2008**, *2*, 2135.
[20] J. Rybczynski, U. Ebels, M. Giersig, *Colloids Surf. A* **2003**, *219*, 1.
[21] Y. Wang, X. Wang, J. Rybczynski, D. Z. Wang, K. Kempa, Z. F. Ren, *Appl. Phys. Lett.* **2005**, *86*, 153120.
[22] C. L. Cheung, R. J. Nikolić, C. E. Reinhardt, T. F. Wang, *Nanotechnology* **2006**, *17*, 1339.
[23] H. Hirai, N. Yakura, Y. Seta, S. Hodoshima, *React. Funct. Polym.* **1998**, *37*, 121.
[24] H. Hirai, N. Yakura, *Polym. Adv. Technol.* **2001**, *12*, 724.
[25] S. Pathak, M. T. Greci, R. C. Kwong, K. Mercado, G. K. S. Prakash, G. A. Olah, M. E. Thompson, *Chem. Mater.* **2000**, *12*, 1985.
[26] T. C. Wei, C. C. Wan, Y. Y. Wang, C. M. Chen, H. S. Shiu, *J. Phys. Chem. C* **2007**, *111*, 4847.

© 2011 WILEY-VCH Verlag GmbH & Co. KGaA, Weinheim